Multi-objective Design Optimization of an IPMSM Based on Multilevel Strategy

Xiaodong Sun, *Senior Member, IEEE*, Zhou Shi, Gang Lei, *Member, IEEE*, Youguang Guo, *Senior Member, IEEE*, and Jianguo Zhu, *Senior Member, IEEE*

***Abstract*— The multi-objective optimization design of interior permanent magnet synchronous motors (IPMSMs) is a challenge due to the high dimension and huge computation cost of finite element analysis. This paper presents a new multilevel optimization strategy for efficient multi-objective optimization of an IPMSM. To determine the multilevel optimization strategy, Pearson correlation coefficient analysis and cross-factor variance analysis techniques are employed to evaluate the correlations of design parameters and optimization objectives. A three-level optimization structure is obtained for the investigated IPMSM based on the analysis results, and different optimization parameters and objectives are assigned to different levels. To improve the optimization efficiency, Kriging model is employed to approximate the finite element analysis for the multi-objective optimization in each level. It is found that the proposed method can provide optimal design schemes with a better performance like smaller torque ripple and lower power loss for the investigated IPMSM, while the needed computation cost is reduced significantly. Finally, experimental results based on a prototype are provided to validate the effectiveness of the proposed optimization method. The proposed method can be applied for efficient multi-objective optimization of other electrical machines with high dimensions.**

***Index Terms*—Multi-objective optimization, Multilevel optimization, Pearson correlation coefficient analysis, Cross-factor variance analysis, finite element analysis, Interior permanent magnet synchronous motor (IPMSM).**

I. INTRODUCTION

Recently, the rapid development of electric vehicles (EVs) has put forward the design optimization researches of different types of electrical machines including the permanent magnet (PM) synchronous motors (PMSMs) [1-7]. As EVs face complex road conditions, the design requirements and optimizations objectives of EV drive motors are complicated compared with those conventional motors. Many factors need to be considered in the design and optimization progress, such as average torque, torque ripple, cogging torque, core loss, efficiencies at different working points, rotor mechanical strength, and temperature rise [8-11].

The design optimization of electrical machines is a nonlinear problem. Thus, it is difficult to establish an accurate mathematical model to evaluate and optimize the performance. Finite element model (FEM) is often used in the design and optimization progress. In [12], a high-power circular winding brushless DC motor was optimized through large-scale design parameter sweeping, and the best type of slot-pole combination and the best design scheme were selected and validated by using FEM simulation. Moreover, a multifactor regression analysis was performed to establish the relationship between performance objectives and design parameters. In [13], an interior permanent magnet synchronous motor (IPMSM) for wide constant-power region operation was optimized by using a new algorithm. In [14], all the structural parameters of a permanent magnet synchronous generators were optimized by using dual-level response surface methodology and Booth's algorithm. These studies have carried out a comprehensive optimization of a number of structural parameters to obtain several optimization objectives.

The conventional optimization methods require huge computation cost of FEM when the dimension of the optimization problem is high, for example, more than 10. To reduce the computation cost, multilevel optimization methods have been developed by dividing the high-dimensional design problem into several low-dimensional subspace optimization problems. There are two main kinds of multilevel optimization methods. One is the multilevel genetic algorithm (MLGA) method. In [15], a multilevel optimization problem was described by using the problem matrix to optimize a PMSM.

Manuscript received July 08, 2019; revised September 06, 2019; accepted December 19, 2019. This work was supported by the National Natural Science Foundation of China under Project 51875261, the Natural Science Foundation of Jiangsu Province of China under Projects BK20180046 and BK20170071, the "Qinglan project" of Jiangsu Province, the Key Project of Natural Science Foundation of Jiangsu Higher Education Institutions under Project 17KJA460005, the Six Categories Talent Peak of Jiangsu Province under Pro-ject 2015-XNYQC-003, the Postgraduate Research & the Practice Innovation Program of Jiangsu Province under Project KYCX17_1815, and the State Scholarship Fund of China Scholarship Council under Grant 201908320298. (*Corresponding author: Gang Lei*.)

X. Sun and Z. Shi are with the Automotive Engineering Research Institute, Jiangsu University, Zhenjiang 212013, China (email: xdsun@ujs.edu.cn, shizhoujiangda@163.com).

G. Lei and Y. Guo are with the School of Electrical and Data Engineering, University of Technology Sydney, NSW 2007, Australia (e-mail: Gang.Lei@uts.edu.au, Youguang.Guo-1@uts.edu.au).

J. Zhu is with the School of Electrical and Information Engineering, University of Sydney, NSW, 2006, Australia (e-mail: jianguo.zhu@sydney.edu.au).

The values in the problem matrix were deduced by correlation analysis. Besides, the architecture and implementation of MLGA were carried out. The other method is the multilevel optimization method based on sensitivity analysis. Multiple motor structure parameters were divided into several optimization levels based on the sensitivity analysis, and these levels will be optimized sequentially till convergence [16-19]. It can be concluded that multilevel optimization has a significant effect on improving the efficiency of motor optimization.

However, these multilevel optimization methods have not investigated the following problems. First, the correlations or mutual sensitivities among different design parameters have not been investigated in the optimization. For example, the sensitivities of PM width and height are calculated separately, and their mutual sensitivities on the torque are quite different. If the conventional local sensitivity analysis is used, these two parameters may be assigned to two different levels. Obviously, they are highly correlated and should be allocated to one level. Second, in previous studies, only the correlation between optimization parameters and objectives has been concerned, while the correlation among different optimization objectives has not been analyzed. In this research, the optimization parameters and optimization objectives will be classified theoretically by using the Pearson correlation coefficient analysis and cross-factor variance analysis based on the design of experiments (DOE) technique. Third, in previous multilevel optimization studies, only one optimization objective is set for each optimization level. When multiple objectives need to be optimized in each level of the optimization, only Pareto solutions can be obtained without specific parameters, which makes traditional methods unable to use. To solve this problem, three key points of solutions which have a certain distance from each other are selected from the Pareto solution of each level, and they will be brought into the next level optimization. Then, the Pareto solutions of three points will be combined to acquire a comprehensive Pareto solution. In this way, the multi-objective optimization of each level can be basically guaranteed, and the final optimization results can be obtained.

This paper aims to develop a new multilevel optimization strategy for the multi-objective optimization of an IPMSM by using Pearson correlation coefficient analysis and cross-factor variance analysis. The remainder of the paper is organized as follows. Section II shows the parametrized FEM and Pearson correlation coefficient analysis for the IPMSM. Section III presents the flowchart and details for the multilevel optimization of this IPMSM. Section IV shows the Pareto optimal solutions of each optimization level and discusses the selection method of a final optimal design. Section V shows the experimental results on a prototype and the comparisons between simulated and measured results, followed by the conclusion.

II. Parametrized FEM for the IPMSM and Pearson Correlation Coefficient Analysis

A. Parametrized FEM and Parameter classification

The FEM of a 48-slot 8-pole IPMSM motor with single-layer V-type sintered Nd-Fe-B magnets has been set up in ANSYS Maxwell. The parameterized cross-section in Fig. 1 includes 16 design parameters, which are rationalized and confined according to Table I. These geometric parameters can be further classified into several types. The first type is the initial design parameters. The stator outer and rotor inner radii are fixed to 100 and 22.5 mm, respectively. They are determined by the initial design of the motor. Tooth width (W_T) and bridge length (L_B) are the parameters which are related to the rotor structural strength closely. These two parameters are closely related to magnetic flux leakage. In the process of electromagnetic finite element optimization, the motor with smaller tooth width and bridge length will show better electromagnetic performance. However, these two parameters cannot be too small due to the limitation of rotor mechanical strength. Therefore, their minimum sizes satisfying the strength can be calculated in the design process without complicated optimization calculation. They are determined to be 1 mm and 1.57 mm, respectively, in this work. The permanent magnet (PM) height (h_{pm}) is closely related to the demagnetization performance of PMs. A relative small thickness h_{pm} will lead to the demagnetization of the motor, thereby reducing the reliability of the motor. Hence, h_{pm} is not suitable for optimization, so it is determined to be 6.07 mm.

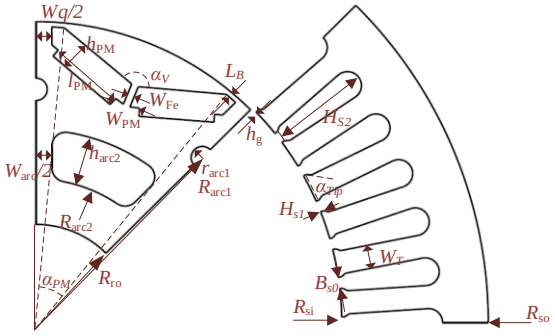

Fig. 1. Parameterized model of the studied IPMSM motor.

TABLE I
INITIAL DESIGN PARAMETERS OF THE IPMSM

	Par.	Description	Unit	Range/Value
Stator and air gap	R_{so}	Stator outer radius	mm	100
	R_{si}	Rotor outer radius	mm	60-70
	H_{s1}	Slot opening depth	mm	0.5-1.2
	H_{s2}	Slot depth	mm	17-22
	B_{s0}	Slot opening width	mm	1.5-3.5
	W_T	Tooth width	mm	3-5
	α_{Tip}	Tooth tip angle	deg	20-45
	h_g	Air gap length	mm	0.5-2
Rotor	L_B	Bridge length	mm	1
	W_{Fe}	Magnet post	mm	1.57
	h_{pm}	PM height	mm	6
	l_{pm}	PM length	mm	7-9
	$8*\alpha_{pm}$	Pole angle	deg	128-136

	α_V	V shape angle	deg	130-160
	W_q	Web width	mm	5-7
	R_{ro}	Rotor inner radius	mm	22.5

B. Optimization objectives

The main design optimization objectives of an EV drive motor are described as follows.

1) Direct objectives:

Vehicle drive motors put forward many requirements for motor performance, including the rated torque, maximum torque, rated point efficiency, torque ripple, and continuous working capacity. Some of these parameters can be obtained directly by simple electromagnetic field simulation, and the others need further calculation.

2) Indirect objectives:

In the process of motor optimization design, some indirect parameters are also selected as the optimization objectives, such as the air gap magnetic flux density, back-EMF, and *d-q* axis inductance. These parameters are closely related to the performance of the motor.

Obviously, these optimization objectives are not completely independent. For example, there is a significant positive correlation between back EMF and torque. On the other hand, there is no strong connection between some of these objectives. Reasonable selection of optimization objectives can not only reduce the number of models which need to be calculated but also improve the efficiency of optimization.

Through preliminary analysis, the maximum torque under determined current density, torque ripple at rated working point (T_{rip}%), total loss at rated work point (P_{rated}), and back-EMF harmonic distortion (*Har*%) are chosen as the optimization objectives.

C. Pearson correlation coefficient analysis

After the initial design and selection of the optimized objectives, a comprehensive sensitivity analysis method is adopted to evaluate the influence of each design parameter on different design objectives. In previous studies, sensitivity analysis of all design parameters and optimization objectives has always been carried out. However, when the number of these design parameters and optimization objectives increases, it is time-consuming to finish the optimization. Meanwhile, the sensitivity results depend on the initial design, and this is a disadvantage of the conventional local and global sensitivity analysis methods.

In the aspect of the selection of correlation coefficients, Pearson, Spearman, and Kendall analysis methods are commonly used. As the linear relationship between the design parameters and design objectives is mainly presented in this study, Pearson correlation coefficient is the most suitable for this study which can be given by:

$$\rho_{X_i,Y_i} = \frac{N\sum X_i Y_i - \sum X_i \sum Y_i}{\sqrt{N\sum X_i^{\,2} - (\sum X_i)^2}\sqrt{N\sum Y_i^2 - (\sum Y_i)^2}} \quad (1)$$

where Y_i is the *i*-th optimization objective, X_i is the design parameters, and N is the sample size.

In the implementation, a DOE technique is first used to generate some samples (like four or five levels for each design parameter) which can cover more information about the whole design space. Then, the correlation coefficients of the parameters to the optimization objectives are calculated based on the FEM results of those samples. Therefore, the obtained results will not be affected by the initial design and can overcome the disadvantages of the conventional local/global sensitivity analysis methods.

The sensitivities of all stator and rotor design parameters on the optimization objectives can be calculated based on (1), as shown in Figs. 2-3. As shown, the Pearson correlation coefficients of the stator and rotor parameters are separated which is mainly due to that the optimization of stator and rotor has certain independence, and the influence of parameters on stator and rotor are relatively low. Besides, as the stator parameters mainly affect the stator iron loss, while the PM eddy loss is the main part of the rotor loss. In [20-23], it was pointed out that taking rotational core loss into account can improve the estimation accuracy of the electric machine core losses and the effects of pulsating, elliptically and circularly rotational losses in a tooth body for a given slot-pitch were examined. Furthermore, the copper loss is mainly caused by winding structure, copper wire size and other factors. The influence of copper loss can be ignored in this study because these factors are fixed in the optimization progress. Therefore, it may be more advisable to analyze stator iron loss for stator parameters and PM eddy loss for rotor than to analyze total loss for both parts.

The Pearson correlation coefficients of different optimization objectives are listed in Table II. -Max torque is adopted in the Pearson correlation coefficient analysis to ensure that all objectives are aimed to be minimal in the optimization. As shown, the Pearson correlation coefficient between harmonic distortion and torque ripple is 0.91, which means that the two optimization objectives are highly positively correlated. Besides, the Pearson correlation coefficient between -max torque and other optimization objectives are negative, which means contradictions among the objective of optimizing -max torque and other optimization objectives. These results of Pearson correlation coefficients among different optimization objectives also show the necessity of multi-objective optimization.

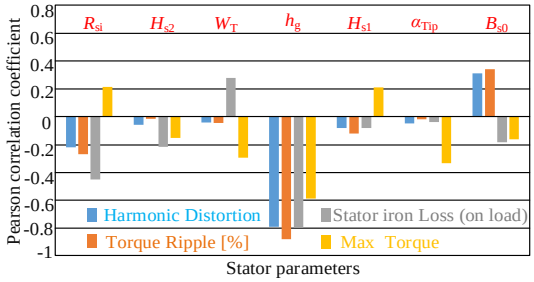

Fig. 2. The Pearson correlation coefficient of the stator parameters to the four optimization objectives.

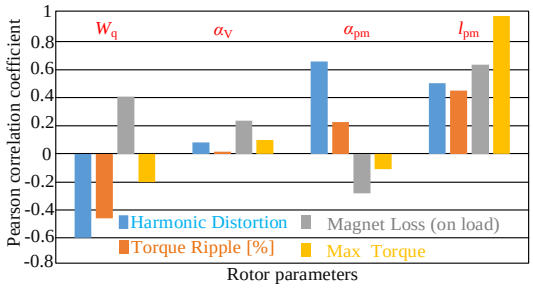

Fig. 3. The Pearson correlation coefficient of the rotor parameters to the four optimization objectives.

TABLE II
PEARSON CORRELATION COEFFICIENTS OF THE OPTIMIZATION OBJECTIVES

PEARSON	Harmonic distortion	Torque ripple	-Max torque	Stator iron loss	Magnet loss
Harmonic distortion [%]	1	0.91	-0.489	0.572	0.289
Torque ripple [%]	0.91	1	-0.651	0.639	0.092
-Max torque [Nm]	-0.489	-0.651	1	-0.576	0
Stator iron loss [W]	0.572	0.639	-0.576	1	0.595
Magnet loss [W]	0.289	0.092	0	.595	1

D. Cross-factor variance analysis

Pearson correlation coefficient analysis can evaluate the influence of each design parameter on different design objectives. The relationship among different optimization objectives can also be achieved through the Pearson correlation coefficient analysis. However, two parameters may be highly correlated with each other while one has a higher correlation coefficient, and the other has a low correlation coefficient. In this case, dividing these two parameters into two optimization levels is clearly inappropriate.

To deal with this problem, cross-factor variance analysis is adopted in this study. First, a new DOE, which can deal with the cross-factor variance analysis, needs to be carried out. Unlike the analysis of variance, interaction can be considered as an independent factor in the DOE of multivariate variance analysis. Assuming that each factor and interaction are independent, interaction can be arranged into a special column in the DOE interaction table.

Second, analysis of the cross-factor variance based on the new DOE and the ***F***-test result will be used to show the correlation effects. The cross-factor variance and ***F***-test can be given by

$$s_k^{\,2} = \frac{U_k}{a_k - 1} \qquad s_e^{\,2} = \frac{Q}{\prod_{k=1}^{k} (a_k - 1)} \tag{2}$$

$$F_k = \frac{s_k^{\,2}}{s_e^{\,2}} \tag{3}$$

where s_k^2 is the variance of the k-th column element, s_e^2 is the variance of random error, Q is the square of deviance, F_k is the ***F***-test result of k-th column element, and (a_k-1) is the degree of freedom of k-th column element.

Finally, ***F***-test will be taken to select the cross-factors which are significant to the optimization objectives. The screening criteria are as follows:

$$F_k \geq F_{0.05,\,(a_k-1,\,a_e-1)} \tag{4}$$

where (a_e-1) is the degree of freedom of the random error.

In order to study the interaction of these design parameters, the interaction F_k of rotor parameters, stator parameters and both parameters in stator and rotor which have high Pearson correlation coefficient are carried out. The cross factors which satisfy (4) are listed in Table III.

TABLE III
CROSS-FACTORS WITH SIGNIFICANT INFLUENCE ON THE OPTIMIZATION OBJECTIVES

Optimization objectives	Max torque	Torque ripple	Total loss
Cross factors	(R_{si} ×h_g) (R_{si} ×H_{s2}) (W_T ×H_{s2}) (α_{pm} ×l_{pm}) (W_q ×l_{pm})	(R_{si} ×h_g) (H_{s1} ×α_{Tip}) (α_{pm} ×l_{pm}) (W_q ×l_{pm})	(R_{si} ×h_g) (R_{si} ×H_{s2}) (W_T ×H_{s2})

As shown, there are five cross-factors which have significant influences on the max torque, four significant cross-factors on the torque ripple, and three significant cross-factors on the total loss. There is no cross-factors consisting of one stator parameter and one rotor parameter. This means that the optimization of stator and rotor can be divided into different levels. Besides, most parameters in all cross-factors have high Pearson correlation coefficients. H_{s2} has low Pearson correlation coefficients but it has strong interaction with several other parameters on max torque and total loss. That means that it is necessary to put H_{s2} with other parameters in the same optimization level.

Through the above Pearson correlation coefficient analysis and cross-factor variance analysis, all the optimization parameters can be divided into three optimization levels. They are the significant stator parameters, significant rotor parameters, and non-significant parameters.

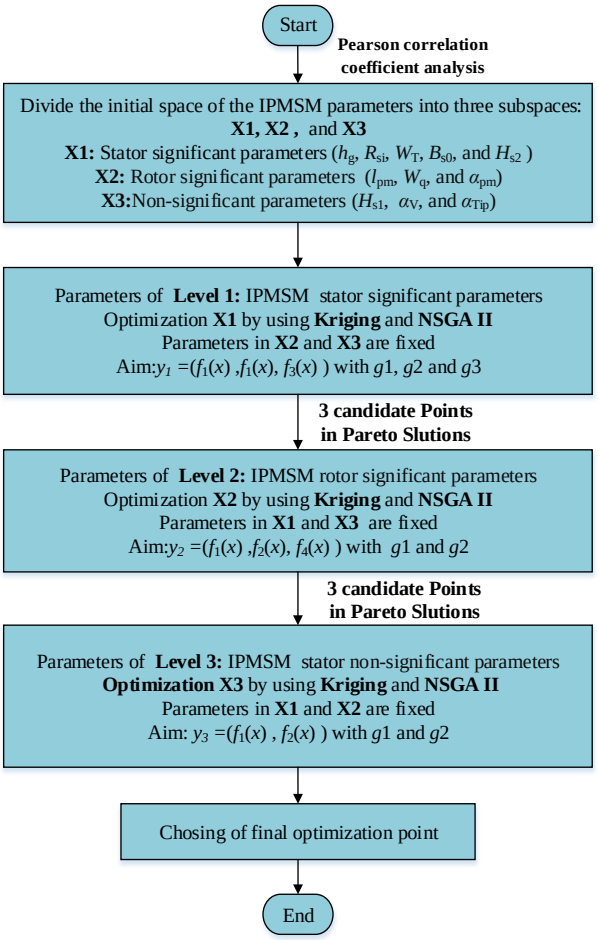

Fig. 4. Multilevel optimization flowchart for IPMSM motor.

III. Multilevel Optimization Method

In this study, the multiple motor structure parameters are involved, and several optimization objectives are considered. If these parameters are optimized in a single level, a large number of sampling FEM points are needed to construct an approximation model like response surface model (RSM). In addition, too many optimization parameters will greatly increase the number of iterations needed in the optimization progress, which will lead to a significant increase in optimization time. Therefore, it is necessary to use a multilevel optimization method.

Fig. 4 shows an optimization framework for the investigated IPMSM based on the multilevel optimization strategy. As shown, the optimization progress has been divided into three levels. Different objectives and constraints will be considered for each optimization level. The objectives are the max torque (T_{max}), torque ripple ($T_{rip\%}$) and total loss (P_{rated}). Harmonic distortion is not selected as the optimization objective because harmonic distortion and torque ripple are highly consistent in all parametric analyses. Therefore, if the torque ripple has been set as one of the optimization objectives, the harmonic distortion can be ignored. The total loss can be divided into the stator iron loss (P_{stator}) and PM loss (P_{PM}), which are much suitable for multilevel optimization. The optimization objectives of this IPMSM can be defined as

$$\min: \begin{cases} f_1(x) = -T_{\max} \\ f_2(x) = T_{rip}\% \\ f_3(x) = P_{\text{stator}} \\ f_4(x) = P_{\text{PM}} \end{cases} \tag{5}$$

Besides, there are several constraints.

$$\begin{cases} g_1(x) = 0.85 - \eta \le 0 \\ g_2(x) = 150 - T_{\max} \le 0 \\ g_3(x) = 85 - S_{\text{slot}} \le 0 \end{cases} \tag{6}$$

where η is the efficiency of the rated working point, and S_{slot} is the slot area of each slot which is decided by the stator parameters. Constraints $g(1)$ and $g(2)$ are valid for each optimization level, while $g(3)$ is only valid for level 1.

Significant parameters of the stator and rotor will be optimized in level 1 and level 2, respectively, in terms of the analysis results listed in Tables II and III. The remaining non-significant parameters will be optimized in level 3. Besides, the optimization objectives and constraints for each level are different. In level 1, the optimization objectives are the max torque, torque ripple, and stator iron loss. In the optimization progress, the slot area should be constrained. While in level 2, the optimization objective stator iron loss is substituted by the PM loss. And in level 3, only the max torque and torque ripple are set as the optimization objectives because these influence of non-significant parameters on the loss are quite low.

By allocating different parameters into different optimization levels and setting different optimization objectives and constraints for each level, the optimization efficiency can be improved significantly.

Multi-objective optimization method is used for all the three optimization levels. For example, regarding the multi-objective optimization of level 1 (stator significant parameters h_g, R_{si}, W_T, B_{s0} and H_{s2}), the optimization objectives are the max torque, torque ripple, and stator core loss. All three constraints are considered in this optimization level. Through the FEM, all the optimization objectives and constraints can be calculated. However, the computational cost of FEM is very high. As an alternative, some approximate models are used in practical engineering design to reduce the computational burden of the optimization process. Kinging model is chosen to construct the approximate multi-objective optimization models to reduce the FEM computation cost of IPMSM in this work. Kriging is a semi-parameter model whose response value incorporates a mean trend term and a variance term as

$$y(x) = y_0(x) + z(x) \tag{7}$$

where $y_0(x)$ can be a RSM, such as linear polynomial and quadratic polynomial, $z(x)$ is the error function which is generally defined as a vector parameter with mean of zero, variance σ^2 and covariance matrix $C_w=[c_{ij}]$ as

$$c_{ij} = \sigma^2 \mathbf{R}\left[R\left(x_i, x_j\right)\right] \quad i, j = 1, 2, \cdots n \tag{8}$$

where x_i and x_j are the sample points, $\mathbf{R}$ is the correlation matrix, and R is a correlation function. Kriging model is claimed to be superior in the modeling of local nonlinearities and has been widely used in the design of electromagnetic devices including electrical machines.

In the multi-objective optimization method, the optimal solutions are actually a compromise among all the objectives.

The Pareto solutions are usually obtained by optimization algorithms. Various optimization algorithms have been applied to the multi-optimization problems, such as multi-objective DEA, non-dominated sorting genetic algorithm (NSGA), and its improved version NSGA II. Among these, NSGA II is one of the most efficient multi-objective evolutionary algorithms and has been widely applied in industrial multi-objective optimization problems.

When the optimization in the first level is completed, three candidate points will be chosen from the Pareto solutions for the multi-objective optimization of the second level. For each candidate point, the second level optimization will be carried out by using the same optimization progress as in level 1. Then three new candidate points will be chosen from the comprehensive Pareto solutions of level 2 optimization for the next level optimization. The same progress will be applied in the level 3 optimization.

TABLE IV
OPTIMIZATION RESULTS OF LEVEL 1

	Par	unit	Point 1-1	Point 1-2	Point 1-3
Level 1 design parameters	H_{s2}	mm	20.1	20.2	20
	W_T	mm	5.9	5.9	4.47
	R_{si}	mm	69.4	68.4	68.8
	h_g	mm	1.53	0.73	1.60
	B_{s0}	mm	2.43	2.05	1.85
Optimization objectives	T_{max}	Nm	180.1	202.1	166.3
	T_{rip}%	%	9.01	16.3	9.6
	P_{stator}	W	261	289	225

IV. OPTIMIZATION RESULTS AND DISCUSSION

A. Optimization Results

Fig. 5 and Table IV show the Pareto solution results of the level 1 optimization of the IPMSM. As shown, the max torque can reach 217 Nm, the torque ripple can reach 7% and the stator core loss can reach 200 W. Three candidate points (Point 1-1, Point 1-2, Point 1-3) are selected from the Pareto solutions whose design parameters and optimization objectives results are given in Table IV.

To ensure the selected points can represent more information of the whole Pareto solutions, they are mainly selected from three ranges (150-170 Nm, 170-190 Nm, and 190-210 Nm) defined by the maximal torque. Also, a certain distance should be applied to them to ensure that the coverage of the next level of optimization is broader. The design parameters of these three candidate points will be used in the level 2 optimization.

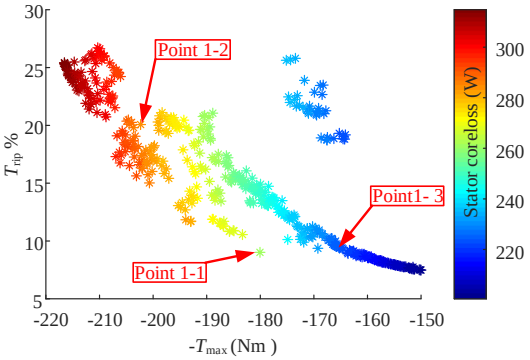

Fig. 5. Pareto solutions of Level 1 optimization.

Fig. 6 and Table V show the Pareto solution results of the level 2 optimization of the IPMSM. As shown in Figs. 6(a)-(c), through the level 2 optimization the Pareto solutions of three candidate points (Point 2-1, Point 2-2, Point 2-3) can be calculated. Besides, the comprehensive Pareto solution results are shown in Fig. 6(d).

The max torque can reach 211 Nm, the torque ripple can reach 3.5% and the PM loss can reach 3.4 W. It is obvious that through the level 2 optimization the max torque and torque ripple are further optimized compared with the candidate points in level 1. Besides, the PM loss has been calculated in this level, and the PM loss of these three candidate points distinguish from each other obviously.

Similarly, three candidate points are selected from the Pareto solutions whose design parameters and optimization objectives results are given in Table V. The design parameters of these three candidate points will be used in the level 3 optimization.

Figs. 7(a)-(c) show the Pareto solution results of the level 3 optimization of the IPMSM. As shown, the influences of design parameters in level 3 on the design objectives are lower than that of levels 1 and 2. Especially, the influence on the max torque is small. The optimization result is consistent with the results of the Pearson correlation coefficient analysis. As the influence on the torque is small, Point 3 is selected as the final optimized point. The final optimization result is shown in Table VI.

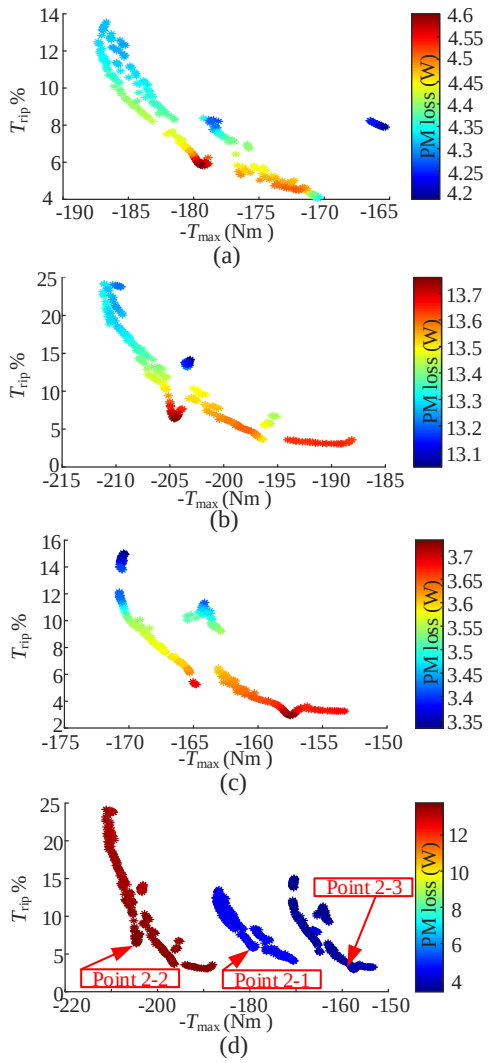

Fig. 6. (a) Pareto solutions of Level 2 point 1-1, (b) Pareto solutions of Level 2 point 1-2, (c) Pareto solutions of Level 2 point 1-3, (d) Comprehensive Pareto solutions of Level 2 optimization.

TABLE V
OPTIMIZATION RESULTS OF LEVEL 2

	Par	unit	Point 2-1	Point 2-2	Point 2-3
Level 1 design parameters	H_{s2}	mm	20.1	20.2	20
	W_T	mm	5.9	5.9	4.47
	R_{si}	mm	69.4	68.4	68.8
	h_g	mm	1.53	0.73	1.60
	B_{s0}	mm	2.43	2.05	1.85
Level 2 design parameters	W_q	mm	6.9	7	6.8
	$8*\alpha_{pm}$	deg	128.0	128.1	128.1
	l_{pm}	mm	16.7	16.6	15.4
Optimization objectives	T_{max}	Nm	180.1	202.1	166.3
	T_{rip}%	%	9.01	16.3	9.6
	P_{stator}	W	261	289	225
	P_{PM}	W	4.58	13.8	3.7

In order to verify the effectiveness of the multilevel optimization and the accuracy of the Kriging model, the maximal torque and total loss distribution of the initial design point and final optimized FEM are analyzed and are shown in Figs. 8 - 10.

As shown in Fig. 8, the maximal torque curve of the final optimized point is higher than that of the initial design point, and the torque ripple of the final optimized point is lower than that of the initial design point. Besides, the maximal torque and the torque ripple of the FEM agree with the optimization results listed in Table V. As shown in Fig. 9, the color of the total loss distribution of the final optimized point is shallower than that of the initial design point which verifies the effectiveness of the optimization on the loss reduction. Fig. 10 shows the efficiency maps of the motor with the initial design and optimized design, respectively. As shown, the area of efficiency over 96% and the maximal torque of the optimized model are larger than those of the initial model. The FEM simulation results prove the effectiveness of the multilevel multi-objective optimization and prove the accuracy of the Kriging model as well.

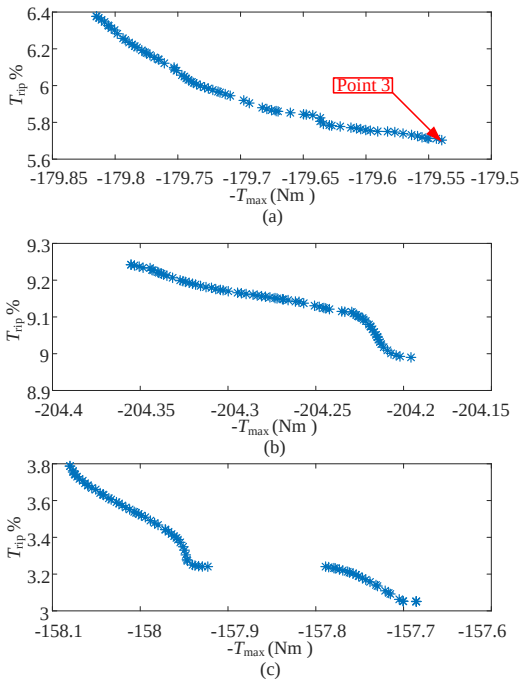

Fig. 7. (a) Pareto solutions of Level 3 point 2-1, (b) Pareto solutions of Level 3 point 2-2, (c) Pareto solutions of Level 3 point 2-3.

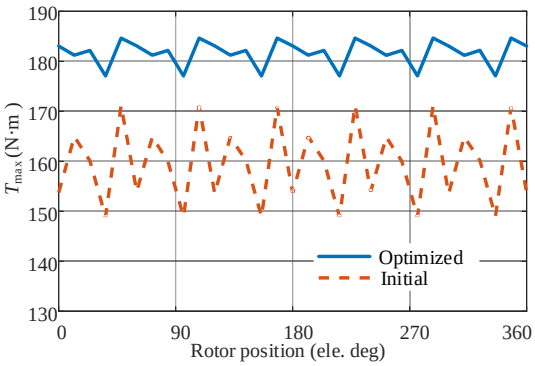

Fig. 8. Comparison of maximal torque curves.

TABLE VI
FINAL OPTIMIZATION RESULTS

	Par.	unit	Initial design	Final optimized
Level 1 design parameters	H_{s2}	mm	20.6	20.1
	W_T	mm	4.2	5.9
	R_{si}	mm	70	69.4
	h_g	mm	1.0	1.53
	B_{s0}	mm	2.5	2.05
Level 2 design parameters	W_q	mm	5.5	6.9
	$8*\alpha_{pm}$	deg	130	128.0
	l_{pm}	mm	15	16.7
Level 3 Design parameters	$Hs1$	mm	0.5	0.67
	α_{Tip}	deg	35	25
	α_V	deg	155	145
Optimization objectives	T_{max}	Nm	160.5	179.5
	T_{rip}%	%	13.4	4.2
	P_{stator}	W	280.4	257
	P_{PM}	W	9.37	4.32

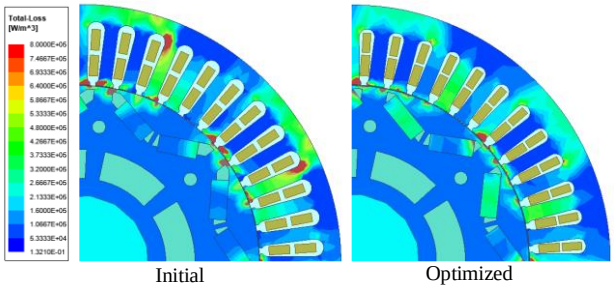

Fig. 9. Comparison of total loss distribution.

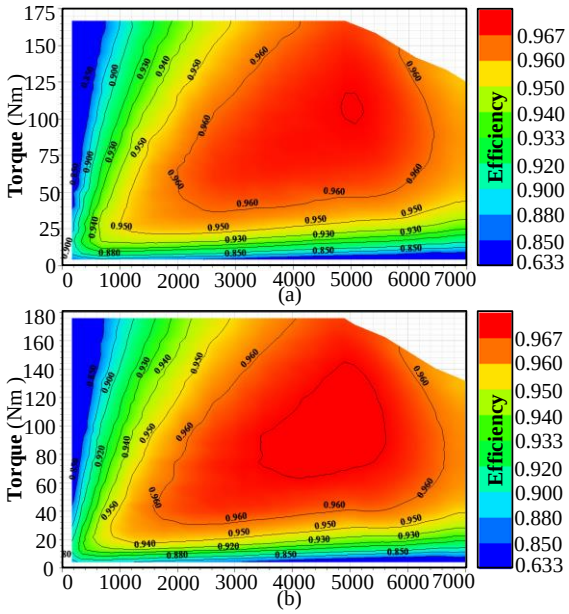

Fig. 10. Comparison of efficiency maps, (a) initial design model, and (b) optimized model.

B. Discussions on computational complexity

In this study, the optimization efficiency can be greatly improved by using the proposed multilevel optimization and Kriging model.

If all the ten design parameters are optimized in one optimization level and five points are selected for each parameter with full factor DOE, 5^{10} FEMs are needed to create the Kriging model for the conventional multi-objective optimization framework, which requires huge computation cost. However, the multilevel optimization method adopted in this study only needs 3375 ($5^5+5^3+5^3$) FEM samples. Besides, a comprehensive parameter analysis ensures the effectiveness of the optimization.

V. EXPERIMENTAL VALIDATION

According to the optimization results, the IPMSM is manufactured for experimental validation. The prototype motors are shown in Fig. 11. The experimental platform is shown in Fig. 12, where an electric vehicle motor test platform is used to test the performance of the IPMSM prototype. The entire measuring system is mounted on the experimental platform, which consists of the dynamometer to drive the motor at a given speed and provide various load torques and the dynamic torque sensor to measure dynamic torque and speed.

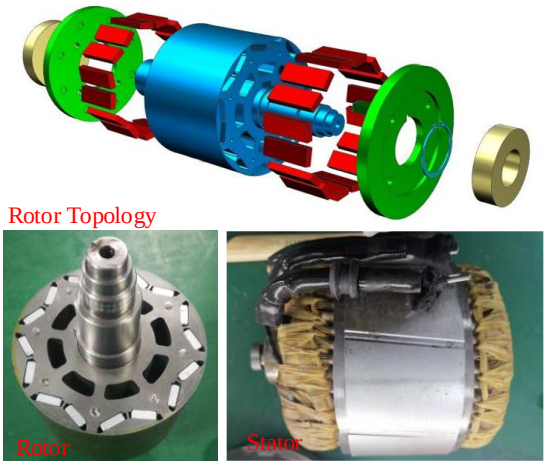

Fig. 11. A prototype of IPMSM.

Fig. 12. Experimental platform.

The measured no-load back-EMF curve of the prototype at 3600 rpm is shown in Fig. 13. As expected, the measured no-load back-EMF of the prototype is nearly the same with the predicted curve of the FEM or FEA (finite element analysis). The torque curves of the proposed model is shown in Fig. 14. The average torque and torque ripple are slightly different, but it can be verified that the torque waveforms of the results of the FEA and the experiment are close.

Besides, the measured efficiency maps in the speed range of 0–6000 rpm are tested and presented in Fig. 15, which is basically consistent with the simulated results in Fig. 9. From the figure, the maximal torque of the prototype could reach 180 Nm, which is in agreement with the predicted max torque of the FEM. And the prototype maintains high efficiency in the main working areas, which meets the design requirements.

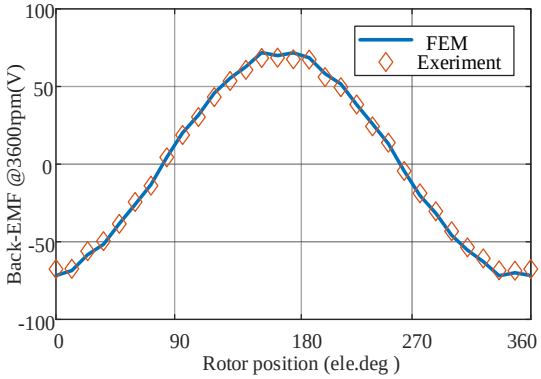

Fig. 13. Measured back-EMF at 3600rpm.

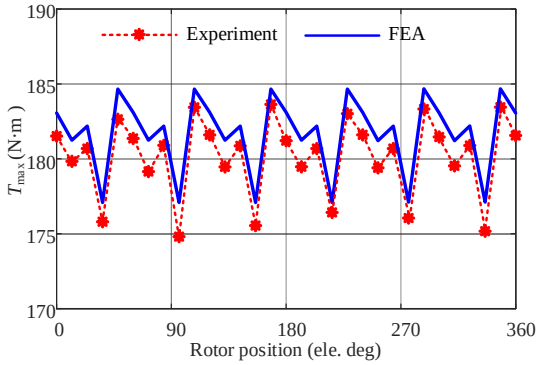

Fig. 14. Measured and FEA maximal torque curves.

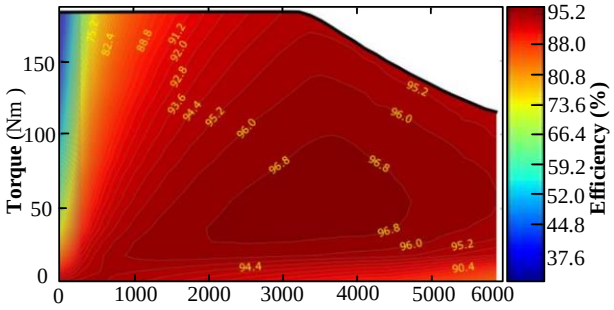

Fig. 15. Measured efficiency maps of the prototype.

VI. Conclusion

A new multilevel optimization strategy for high-dimensional multi-objective optimization design of an IPMSM was presented in this paper. The Pearson correlation coefficient analysis and cross-factor variance analysis were used to analyze the correlations between the design parameters and objectives, which benefited the process of differentiating optimization levels. The proposed correlation analysis method can overcome the disadvantage of conventional local/global sensitivity analysis methods. Based on the correlation analysis results, a three-level optimization was adopted for the optimization of the IPMSM. Besides, Kriging model and NSGA II algorithm were used in the multi-objective optimization of each level. The effectiveness of the multilevel optimization and the accuracy of the Kriging model, as well as the optimization results, were verified by using the FEM results. Through the optimization, the comprehensive efficiency of the IPMSM was effectively improved. Finally, the prototype was tested on an experimental platform. The test results show that the measured results of the prototype agree with the simulation design results. In future work, rotational core loss of this machine will be taken into account to improve the estimation accuracy of the core losses and the optimization model.

References

[1] F. Momen, K. Rahman, and Y. Son, "Electrical propulsion system design of chevrolet bolt battery electric vehicle," *IEEE Trans. Ind. Appl.*, vol. 55, no. 1, pp. 376-384, 2019.

[2] Y. Li, C. Zhu, L. Wu, and Y. Zheng, "Multi-objective optimal design of high-speed surface-mounted permanent magnet synchronous motor for magnetically levitated flywheel energy storage system," *IEEE Trans. Magn.*, pp. 1-8, 2019.

[3] Z. Wang, B. Liu, L. Guan, Y. Zhang, M. Cheng, B. Zhang, and L. Xu, "A dual-channel magnetically integrated EV chargers based on double-stator-winding permanent-magnet synchronous machines," *IEEE Trans. Ind. Appl.*, vol. 55, no. 2, pp. 1941-1953, 2019.

[4] E. Trancho, E. Ibarra, A. Arias, I. Kortabarria, J. Jurgens, L. Marengo, A. Fricassè, and J. V. Gragger, "PM-assisted synchronous reluctance machine flux weakening control for EV and HEV applications," *IEEE Trans. Ind. Electron.*, vol. 65, no. 4, pp. 2986-2995, 2018.

[5] B. Lee, J. Jung, and J. Hong, "An improved analysis method of irreversible demagnetization for a single-phase line-start permanent magnet motor," *IEEE Trans. Magn.*, vol. 54, no. 11, pp. 1-5, 2018.

[6] X. Sun, Z. Shi, L. Chen, and Z. Yang, "Internal model control for a bearingless permanent magnet synchronous motor based on inverse system method," *IEEE Trans. Energy Convers.*, vol. 31, no. 4, pp. 1539-1548, 2016.

[7] X. Sun, C. Hu, G. Lei, Y. Guo, and J. Zhu "State feedback control for a PM hub motor based on Grey wolf optimization algorithm," *IEEE Trans. Power Electron.* vol. 35, no. 1, pp. 1136-1146, 2020.

[8] A. J. Sorgdrager, R. Wang, and A. J. Grobler, "Multiobjective design of a line-start PM motor using the Taguchi method," *IEEE Trans. Ind. Appl.*, vol. 54, no. 5, pp. 4167-4176, 2018.

[9] A. Sarikhani and O. A. Mohammed, "Multiobjective design optimization of coupled pm synchronous motor-drive using physics-based modeling approach," *IEEE Trans. Magn.*, vol. 47, no. 5, pp. 1266-1269, 2011.

[10] M. Ashabani and Y. A. I. Mohamed, "Multiobjective shape optimization of segmented pole permanent-magnet synchronous machines with improved torque characteristics," *IEEE Trans. Magn.*, vol. 47, no. 4, pp. 795-804, 2011.

[11] X. Sun, Z. Jin, S. Wang, Z. Yang, K. Li, Y. Fan, and L. Chen, "Performance improvement of torque and suspension force for a novel five-phase BFSPM machine for flywheel energy storage systems," *IEEE Trans. Appl. Supercon.*, vol. 29, no. 2, pp. 1-5, 2019.

[12] Q. Zhang, S. Cheng, D. Wang, and Z. Jia, "Multiobjective design optimization of high-power circular winding brushless DC motor," *IEEE Trans. Ind. Electron.*, vol. 65, no. 2, pp. 1740-1750, 2018.

[13] F. Parasiliti, M. Villani, S. Lucidi, and F. Rinaldi, "Finite-element-based multiobjective design optimization procedure of interior permanent magnet synchronous motors for wide constant-power region operation," *IEEE Trans. Ind. Electron.*, vol. 59, no. 6, pp. 2503-2514, 2012.

[14] P. Asef, R. B. Perpiñà, M. R. Barzegaran, A. Lapthorn, and D. Mewes, "Multiobjective design optimization using dual-level response surface methodology and booth's algorithm for permanent magnet synchronous generators," *IEEE Trans. Energy Convers.*, vol. 33, no. 2, pp. 652-659, 2018.

[15] S. Wang, X. Meng, N. Guo, H. Li, J. Qiu, J. G. Zhu, Y. Guo, D. Liu, Y. Wang, and W. Xu, "Multilevel optimization for surface mounted PM machine incorporating with FEM, " *IEEE Trans. Magn.*, vol. 45, no. 10, pp. 4700-4703, 2009.

[16] X. Meng, S. Wang, J. Qiu, Q. Zhang, J. G. Zhu, Y. Guo, and D. Liu, "Robust multilevel optimization of PMSM using design for six Sigma," *IEEE Trans. Magn.*, vol. 47, no. 10, pp. 3248-3251, 2011.
[17] G. Lei, C. Liu, J. Zhu, and Y. Guo, "Techniques for multilevel design optimization of permanent magnet motors," *IEEE Trans. Energy Convers.*, vol. 30, no. 4, pp. 1574-1584, Dec 2015.
[18] S. Wang, X. Meng, N. Guo, H. Li, J. Qiu, J. G. Zhu, Y. Guo, D. Liu, Y. Wang, and W. Xu, "Multilevel optimization for surface mounted PM machine incorporating with FEM," *IEEE Trans. Magn.*, vol. 45, no. 10, pp. 4700-4703, 2009.
[19] G. Lei, W. Xu, J. Hu, J. Zhu, Y. Guo, and K. Shao, "Multilevel design optimization of a FSPMM drive system by using sequential subspace optimization method," *IEEE Trans. Magn.*, vol. 50, no. 2, pp. 685-688, 2014.
[20] J. G. Wanjiku, N. Alatawneh, and P. Pillay, "The effect of tooth-width on the distribution of rotational core losses," in *Proc. 2013 Int. Electric Machines & Drives Conf.*, 2013, pp. 594-601.
[21] J. C. Akiror, J. Wanjiku, P. Pillay, J. Cave, and A. Merkhouf, "Rotational core loss magnetizer: design and measurements," *IEEE Trans. Ind. Appl.*, vol. 54, no. 5, pp. 4355-4364, 2018.
[22] Y. G. Guo, J. G. Zhu, J. Zhong, H. Lu, and J. X. Jin, "Measurement and modeling of rotational core losses of soft magnetic materials used in electrical machines: a review," *IEEE Trans. Magn.*, vol. 44, no. 2, pp. 279-291, 2008.
[23] Y. G. Guo, J. G. Zhu, H. Y. Lu, Y. J. Li, and J. X. Jin, "Core loss computation in a permanent magnet transverse flux motor with rotating fluxes," *IEEE Trans. Magn.*, vol. 50, no. 11, art. 6971480, 2014.

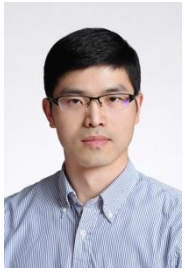

Xiaodong Sun (M'12-SM'18) received the B.Sc. degree in electrical engineering, and the M.Sc. and Ph.D. degrees in control engineering from Jiangsu University, Zhenjiang, China, in 2004, 2008, and 2011, respectively.

Since 2004, he has been with Jiangsu University, where he is currently a Professor with the Automotive Engineering Research Institute. From 2014 to 2015, he was a Visiting Professor with the School of Electrical, Mechanical, and Mechatronic Systems, University of Technology Sydney, Sydney, Australia. His current teaching and research interests include electrical machines and drives, drives and control for electric vehicles, and intelligent control. He is the author or coauthor of more than 90 refereed technical papers and one book, and he is the holder of 36 patents in his areas of interest.

Zhou Shi was born in Nantong, Jiangsu, China, in 1993. He received the B.S. degree in vehicle engineering from Jiangsu University, Zhenjiang, China, in 2016, and he is currently working toward the Ph.D. degree in Jiangsu University, Zhenjiang, China.

His current research interests include design, optimization, magnetic equivalent circuits modeling, control, and loss analysis of permanent magnet synchronous motors for automobile application.

Gang Lei (M'14) received the B.S. degree in Mathematics from Huanggang Normal University, China, in 2003, the M.S. degree in Mathematics and Ph.D. degree in Electrical Engineering from Huazhong University of Science and Technology, China, in 2006 and 2009, respectively. He is currently a senior lecturer at the School of Electrical and Data Engineering, University of Technology Sydney (UTS), Australia. His research interests include design optimization and control of electrical drive systems and renewable energy systems.

Youguang Guo (S'02-M'05-SM'06) received the B.E. degree from Huazhong University of Science and Technology, China in 1985, the M.E. degree from Zhejiang University, China in 1988, and the Ph.D. degree from University of Technology, Sydney (UTS), Australia in 2004, all in electrical engineering. He is currently a Professor at the School of Electrical and Data Engineering, University of Technology Sydney (UTS). His research fields include measurement and modeling of properties of magnetic materials, numerical analysis of electromagnetic field, electrical machine design optimization, power electronic drives and control.

Jianguo Zhu (S'93–M'96–SM'03) received the B.E. degree in 1982 from Jiangsu Institute of Technology, Jiangsu, China, the M.E. degree in 1987 from Shanghai University of Technology, Shanghai, China, and the Ph.D. degree in 1995 from the University of Technology Sydney (UTS), Sydney, Australia, all in electrical engineering. He was appointed a lecturer at UTS in 1994 and promoted to full professor in 2004 and Distinguished Professor of Electrical Engineering in 2017. At UTS, he has held various leadership positions, including the Head of School for School of Electrical, Mechanical and Mechatronic Systems and Director for Centre of Electrical Machines and Power Electronics. In 2018, he joined the University of Sydney, Australia, as a full professor and Head of School for School of Electrical and Information Engineering. His research interests include computational electromagnetics, measurement and modelling of magnetic properties of materials, electrical machines and drives, power electronics, renewable energy systems and smart micro grids.